[7]H. W. Jackson and E. Feenberg, Rev. Mod. Phys. **34**, 686 (1962).

[8]C.-W. Woo, H. T. Tan, and W. E. Massey, Phys. Rev. **185**, 287 (1969).

[9]C. E. Campbell and M. Schick, Phys. Rev. A **3**, 691 (1971); and M. D. Miller, C.-W. Woo, and C. E. Campbell, Phys. Rev. A **6**, 1942 (1972).

[10]R. L. Coldwell and C.-W. Woo (unpublished).

[11]In a calculation to be reported elsewhere, one of us (M. D. M.) has been unable to reproduce the bulk-helium results reported by W. P. Francis, G. V. Chester, and L. Reatto [Phys. Rev. A **1**, 86 (1970)]. The BBGKY integral equation was employed rather than the PY2XS used by Francis, Chester, and Reatto.

[12]Even if the small-ν (< 0.2 Å^{-1}) corrections to $S(\nu)$ were omitted altogether the effect on the specific heat would be negligible except at the lowest temperatures (<0.5 °K). By introducing the linear extrapolation, one depresses the value of the specific-heat integrand, Eq. (14), at small ν and consequently reduces the specific heat. As the temperature is raised, the intermediate region of the spectrum makes increasingly appreciable contributions to the specific-heat integrand and quickly tends to dominate the effect of the linear region. At $n = 0.036$ Å^{-2}, for example, the heat capacity per unit area (cf., Fig. 5) at $T = 0.1$ °K is 0.11×10^{-3} Å^{-2}; without the linear extrapolation it is 0.24×10^{-3} Å^{-2}. At $T = 0.5$ °K, the heat capacity with the linear extrapolation is 0.152×10^{-2} Å^{-2} and without it is 0.155×10^{-2} Å^{-2}. For $T > 1$ °K the differences are imperceptible. Thus, we can expect that the specific heat will be rather insensitive to a detail such as the proper connection between the small-ν and intermediate-ν regions of $S(\nu)$.

[13]J. G. Dash (private communication).

[14]M. Schick and C. E. Campbell, Phys. Rev. A **2**, 1591 (1970).

[15]C.-W. Woo, J. Low Temp. Phys. **3**, 335 (1970).

[16]See, for example, D. R. Hartree, *The Calculation of Atomic Structures* (Wiley, New York, 1957), p. 71; and F. Herman and S. Skillman, *Atomic Structure Calculations* (Prentice-Hall, Englewood Cliffs, N. J., 1963).

PHYSICAL REVIEW A VOLUME 7, NUMBER 4 APRIL 1973

Pressure Dependence of Self-Generated Magnetic Fields in Laser-Produced Plasmas*

R. S. Bird, L. L. McKee,† F. Schwirzke, and A. W. Cooper
Naval Postgraduate School, Monterey, California 93940
(Received 5 September 1972)

The systematic dependence of the magnitude of the self-generated magnetic fields of a laser-produced plasma on nitrogen background pressure has been investigated. At expansion distances of a few millimeters or more, the strongest fields were found to reside at the front of the streaming laser plasma. Magnetic fields were created in the laser plasma long after laser shut off by allowing the streaming plasma to impinge upon a glass plate.

Magnetic fields spontaneously generated in the absence of applied fields have been observed in several experiments with laser-produced plasmas.[1-3] Stamper *et al.*[3] have suggested that these spontaneous fields result from thermo-electric currents associated with temperature and pressure gradients existing during the early stages of the formation and heating of a plasma by a giant laser pulse.

We have made a systematic study of the dependence of the spontaneous magnetic fields on the pressure of the background gas which indicates that magnetic fields are generated by pressure gradients in the front of the expanding laser plasma. Field amplification or field reversal can be caused by increase or reversal of the pressure gradients in the plasma front long after the end of the laser pulse.

The equation describing the development of the magnetic fields is obtained from the generalized Ohm's law

$$\vec{J} = \sigma [\vec{E} + \vec{V}_e \times \vec{B} + (1/en_e) \nabla P_e] , \qquad (1)$$

where all quantities have their conventional meaning and the subscript e refers to the electron component of that quantity. Solving for $\vec{E}$ and using

$$\nabla \times \vec{E} = -\frac{\partial \vec{B}}{\partial t}$$

gives

$$\frac{\partial \vec{B}}{\partial t} = \nabla \times (\vec{V}_e \times \vec{B}) + \frac{1}{\mu_0 \sigma} \nabla^2 \vec{B} + \frac{k}{en_e} \nabla T_e \times \nabla n_e . \qquad (2)$$

The first two terms on the right-hand side are the flow and diffusion terms. The generation of a magnetic field requires that the last term, the source term $\vec{S}$, be nonzero.

The beam from a 300-MW (7.5 J in 25 nsec) neodymium-doped glass laser was focused by a lens with a 28-cm focal length. The principal targets were aluminum and Mylar discs. The laser irradiation produced a 2-mm hole in the Mylar (disc thickness 0.01 cm) but did not penetrate the aluminum. The laser beam entered a vacuum chamber and struck the target at an angle of 30° with respect to the target normal. The resultant plasma streamed out along the target normal[4] defining a convenient cylindrical-polar coordinate system with the z axis along the target normal, the $\theta = 0°$ line vertically up, and the origin centered on the burn spot. The magnetic field was analyzed with small

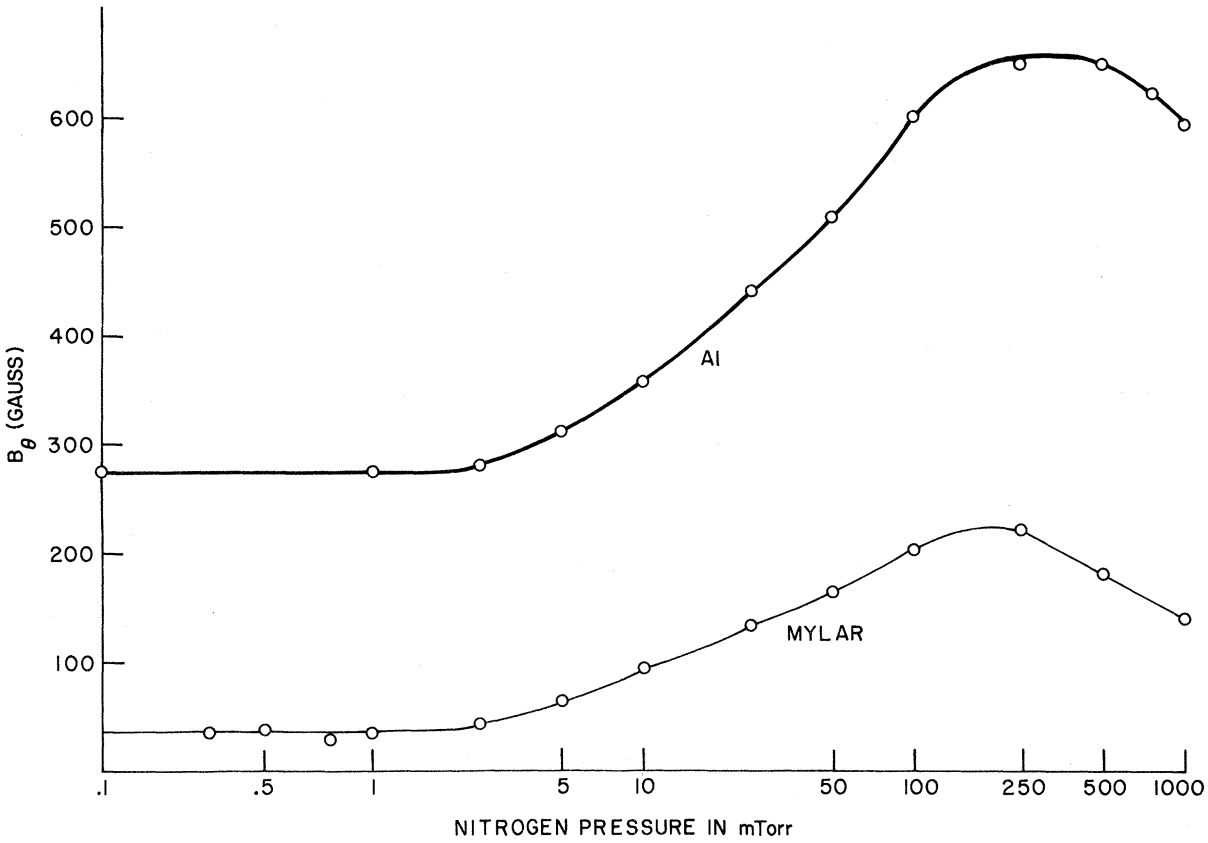

FIG. 1. Maximum azimuthal magnetic field as a function of N_2 background pressure at $r=0.3$ cm, $\theta=0°$, and $z=0.4$ cm for aluminum and Mylar targets.

(~1-mm-diam) inductive probes. Electric double probes were used to study the plasma density variations.

The propagation velocity of the laser plasma front, as determined from the electric-double-probe signals, ranged from about 1.5×10^7 cm/sec at 0.1 mTorr N_2 to 3×10^6 cm/sec at 250 mTorr N_2. These velocities were determined by computing the average velocity of the maximum probe signals along the line $r=0.3$ cm, $\theta=0°$, for z values from 1.0–2.5 cm. The magnetic fields were primarily azimuthal, symmetric about the z axis, and corresponded to an electron current in the $+z$ direction. For pressures above 250 mTorr N_2 and at distances larger than about $z=1$ cm, azimuthal magnetic fields are generated at the front of an expanding aluminum-laser plasma, which are in a direction opposite to the initial fields. This phenomenon is currently under investigation.

Figure 1 displays the manner in which the maximum azimuthal magnetic fields, detected at a fixed position, depend on the background pressure of nitrogen for aluminum and Mylar targets. The pressure at which the magnetic field attains its maximum value was found to decrease as the probe was moved out along the line $r=0.3$ cm, $\theta=0$. At all positions checked (the closest being $r=0.3$ cm, $\theta=z=0$) a pressure dependence was observed. Figure 1 indicates that field amplification depends only on the background gas and that, below about 1 mTorr, the fields are target dependent. The spatial relationship of the magnetic fields to the laser plasma density n_i for an aluminum target and background pressures of 0.1 and 5 mTorr at a time 300 nsec after the arrival of the laser pulse at the target surface is shown in Fig. 2. For the earliest times checked (20 nsec), the maximum fields along this line resided at the front of the expanding laser plasma.

In a previous study,[5] it was observed that, for background pressures above about 30 mTorr, the streaming laser plasma swept up the photoionized background plasma. This snowplowing of the ambient background plasma caused a pileup of the laser plasma. The front thickness δ of the laser plasma was found to scale as the cube root of the background pressure.

The pressure dependence of Fig. 1 shows three regions of behavior. Below about 1 mTorr the fields are pressure independent. In this region the

background plasma density appears to be too small to interact with the laser plasma for the scale lengths of this experiment. In the region above 1 mTorr, the coupling of the background with the laser plasma directly influences the source term of Eq. (2). This influence can be shown by writing the source term $\vec{S} = (k/en_e)\nabla T_e \times \nabla n_e$ in the form $k(\nabla T)_r/e\delta$, where $(\nabla T)_r$ is the radial temperature gradient, here in the negative r direction, and $\nabla n_e/n_e \simeq 1/\delta$. The density gradient is in the negative z direction and δ is characteristic of the length over which the density changes. As the background pressure increases, δ decreases, becoming of the order of the shell thickness at the front of the streaming laser plasma. In the region above 250 mTorr, irreversible dissipation of field energy into particle energy is dominant.

In Fig. 2 the fields for a background pressure of 5 mTorr are larger than those for 0.1 mTorr, with the exception of the region from $z = 1.3$ to $z = 1.5$ cm, where the fields for 0.1 mTorr are slightly larger. Thus it appears that magnetic fields have been created along this line. An order-of-magnitude calculation of the classical diffusion time shows it to be much larger than the experimental time so that the increased field at the front does not appear to be the result of field diffusion, but the result of field generation at the front.

From Eq. (2), it follows that the source term reverses its sign if the direction of the pressure gradient is reversed and it should be possible to create azimuthal magnetic fields, in a direction opposite to the initial fields, by reversing the direction of the pressure gradient at late times in the plasma expansion. Magnetic field reversal has been observed several hundred nanoseconds after shut off of the laser pulse. The field reversal was produced by allowing the expanding laser plasma to impinge upon a glass plate placed at $z = 1.15$ cm. The resulting pileup of the plasma caused a rever-

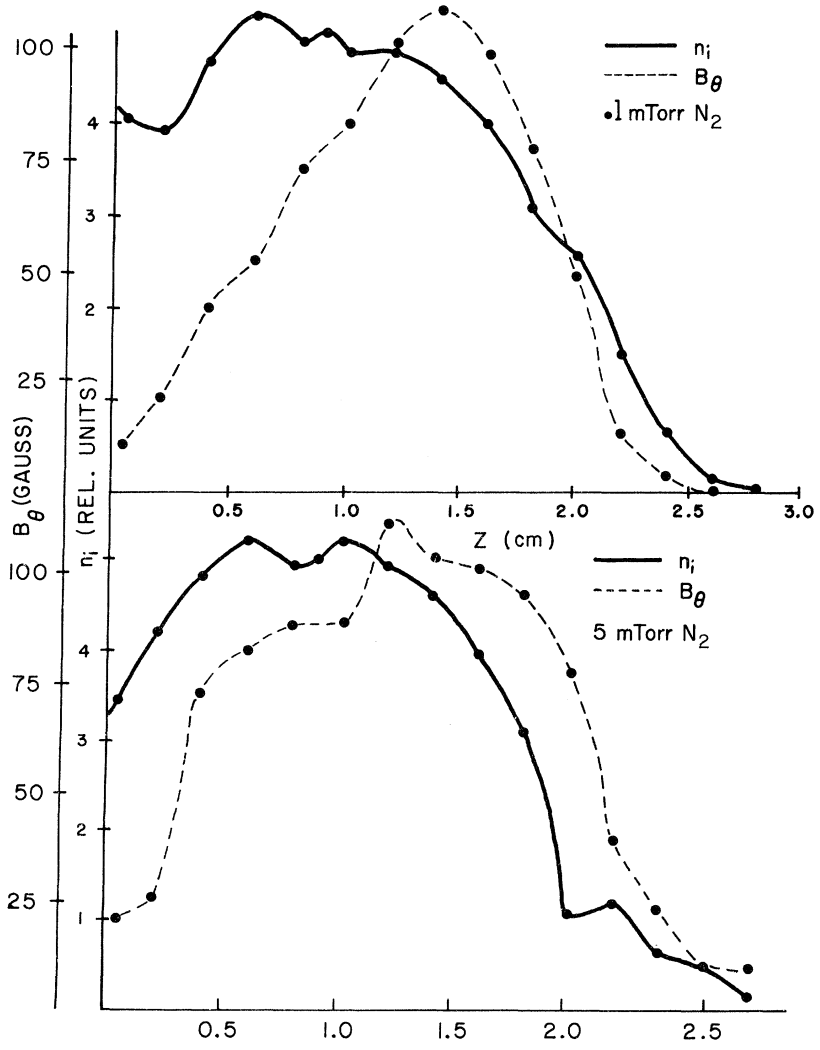

FIG. 2. Relation of B_θ to the plasma density profile n_i along the line $r = 0.3$ cm and $\theta = 0°$, 300 nsec after arrival of the laser pulse, at an aluminum target.

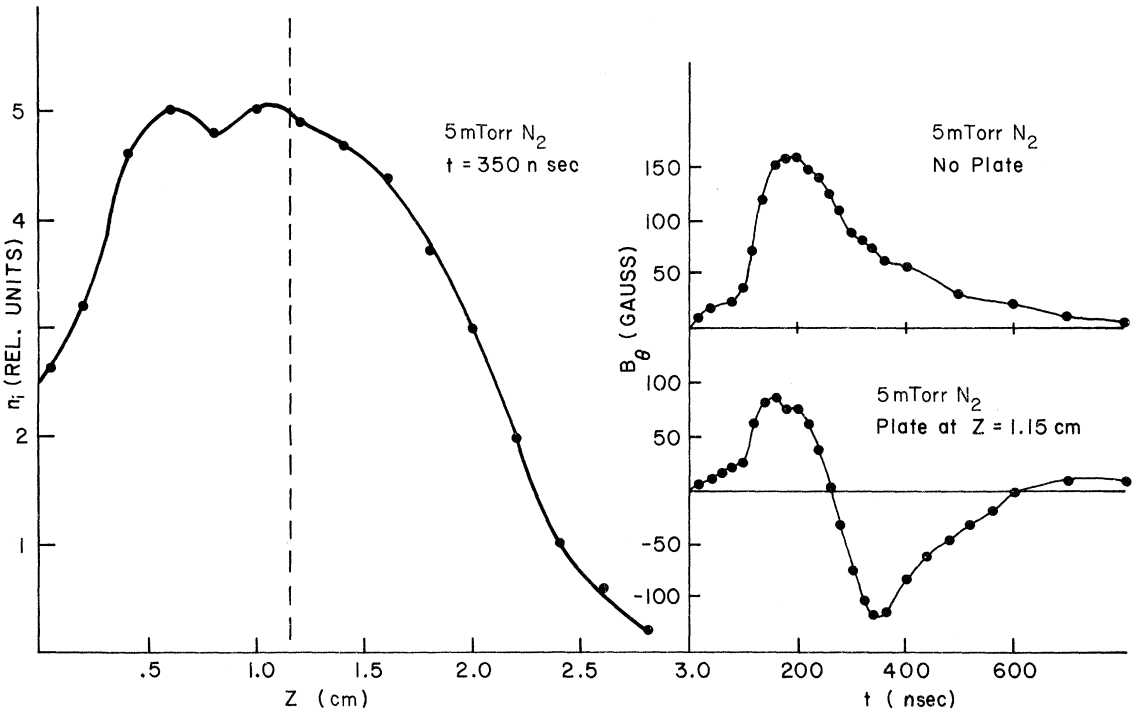

FIG. 3. Plasma density profile along the line $r=0.3$ cm and $\theta=0°$ for an aluminum target; upper-right-hand corner: B_θ at $r=0.3$ cm, $\theta=0°$, $z=1.0$ cm; lower-right-hand corner: B_θ at $r=0.3$ cm, $\theta=0°$, $z=1.0$ cm.

sal of the pressure gradient, a reappearance of the radial temperature gradient, and a corresponding production of azimuthal magnetic fields in a direction opposite to the initial fields. Figure 3 shows the plasma density profile for expansion into a background of 5 mTorr N_2 in the absence of the glass plate. The upper insert shows the azimuthal magnetic fields versus time at the position $r=0.3$ cm, $\theta=0$, $z=1.0$ cm without the glass plate in place, while the lower insert shows the azimuthal fields at the same position but with the glass plate at $z=1.15$ cm and parallel to the target surface. The magnetic field attains its largest negative value at a time $t=350$ nsec, corresponding to the arrival of the front maximum at the plate.

In conclusion, the magnetic fields are found to depend on the background-gas pressure because the background gas influences the pressure gradients in the front of the streaming laser plasma. Also, magnetic fields can be produced long after laser shutoff.

It may be assumed that such a mechanism for the generation of magnetic fields can occur in other streaming plasmas, as for example, in the solar wind encountering the earth's magnetic field.

*Supported by the Air Force Office of Scientific Research under AFOSR Grant No. MPR-0004-69 and by the Office of Naval Research.

†Present address: Air Force Weapons Laboratory, Kirtland A.F.B., New Mexico.

[1]V. N. Korobkin and R. V. Serov, Zh. Eksp. Teor. Fiz. Pis'ma Red. 4, 103 (1966) [Sov. Phys. JETP Lett. 4, 70 (1966)].

[2]G. A. Askar'yan, M. S. Rabinovick, A. D. Smirnova, and V. B. Studenov, Zh. Eksp. Teor. Fiz. Pis'ma Red. 5, 116 (1967) [Sov. Phys. JETP Lett. 5, 93 (1967)].

[3]J. A. Stamper, K. Papadopoulos, R. N. Sudan, S. O. Dean, E. A. McLean, and J. M. Dawson, Phys. Rev. Lett. 26, 1012 (1971).

[4]J. F. Ready, *Effects of High-Power Laser Radiation* (Academic, New York, 1971), p. 165.